

Supplementary materials

Effective Cerebral Tuberculosis Treatment via Nose-to-Brain Transport of Anti-TB Drugs Using Mucoadhesive Nano-aggregates

*Krishna Jadhav¹, Agrim Jhilda¹, Raghuraj Singh¹, Eupa Ray¹, Vimal Kumar², Awadh Bihari
Yadav³, Amit Kumar Singh^{2*} and Rahul Kumar Verma^{1*}*

**Both authors share equal corresponding authorship*

¹Pharmaceutical Nanotechnology lab, Institute of Nano Science and Technology (INST),
Sector-81, Mohali, Punjab, India-160062

²Experimental Animal Facility, ICMR-National JALMA Institute for Leprosy and Other
Mycobacterial Diseases, Tajganj, Agra, India-282004

³Center of Biotechnology. Nehru Science Centre. University of Allahabad. Prayagraj-211002

Correspondence

Dr. Rahul K. Verma, PhD
Scientist-E & Associate Professor
Address: Institute of Nano Science and Technology (INST),
Knowledge city, Sector-81, SAS Nagar, Punjab, INDIA - 140306
Phone Numbers: +91-172-2210073/75 Ext-315, Mobile- +91-8968439969
Fax Number: +91-172-2211074
rahulverma@inst.ac.in

S1. Materials

- **Chemicals and reagents:** Low molecular weight chitosan (degree of deacetylation ~85% and 50000-190000 Daltons), Isoniazid (Batch#0000175711), sodium Tripolyphosphate (TPP), mannitol, Fluorescein isothiocyanate (FITC), 4',6-diamidino-2-phenylindole (DAPI), MTT reagent (3-(4,5-dimethylthiazol-2-yl)-2,5 diphenyl tetrazolium bromide), poly-L-Lysine were obtained from Sigma-Aldrich, USA. Rifampicin (Batch#10559321) was procured as a generous gift sample from Lupin Ltd. India. Isopropyl myristate was procured from SRL chemicals, India. Dulbecco's Modified Eagle's Medium (DMEM), MEM Non-essential Amino acid solution (100X), phosphate buffered saline (PBS), 1X trypsin EDTA solution, Mucin from porcine stomach Type III, 4% Paraformaldehyde solution were procured from Himedia, India. SPLInsert™ Hanging polyethylene terephthalate (PET) culture inserts (4.52 cm² growth area and 0.4 μm membrane pore size) were procured from SPL life sciences, Korea. Fetal Bovine Serum (FBS) and 100X Antibiotic-Antimycotic obtained from Gibco BLR. Purified deionized water was used from a Milli-Q (Millipore, USA) water purification system. All chemicals and reagents were of analytical grade and used as received.
- **Mycobacterial strains:** Virulent *Mycobacterium tuberculosis* C3 strain (MTB C3 strain isolated from the CSF of CNS-TB patients) is maintained in ABSL-3 facility at ICMR-National JALMA Institute for Leprosy & Other Mycobacterial Diseases, Agra (NJIL&OMD), India was used for the generation of mice model of TBM. MTB C3 strain was grown in Middlebrook 7H9 broth (Difco, Detroit, MI, USA) for 28 days with 10% Albumin-dextrose-Catalase (ADC) enrichment, 0.2% glycerol, and 0.05% Tween-80. The plates were cultured at 37°C in an incubator for 3–4 weeks to ascertain the total number of culturable mycobacteria.
- **Cell culture:** Human nasal epithelial cells (RPMI-2650 cell line) was sourced from National Centre for Cell Science (NCCS), India, were grown in Dulbecco's Modified Eagle Medium, containing 10% (v/v) fetal bovine serum, 1% of 1X antibiotic antimycotic solution (100 U/ml penicillin; 100 μg/ml streptomycin; and 2.5 μg/ml amphotericin B), 1X non-essential amino acid solution. Cells were seeded in 25 cm³ and 75 cm³ sterile cell culture flasks under controlled conditions of 37°C and 5% CO₂.

S2. Drug-Compatibility study of Anti-TB drugs with excipients

The combination of different excipients for preparation of nanoformulation necessitate to evaluate the effects of different excipients with drugs. These effects were evaluated by using FT-IR analysis. The FT-IR spectra of INH, RFP, PYR, physical mixture and NPs revealed that all characteristic peaks preserved represents no interaction between drugs and polymers. This study revealed that there were no chemical changes observed between anti-TB drugs and excipients used for nanoparticles preparation. The characteristic peaks of INH [3300 cm^{-1} (N-H stretching, Amine), 3108 cm^{-1} (C-H asymmetric stretching), 3008 cm^{-1} (C-H sym stretching), 1664 cm^{-1} (C=O stretching), 1552 cm^{-1} (N-H bending), 1327 cm^{-1} (NH_2 wagging)], RFP [3483.85 cm^{-1} (ν (-NH)), 2975 cm^{-1} (ν (-OH)), 1648 cm^{-1} (ν (-C=O)), 1567 cm^{-1} (amide C=O), 1726 cm^{-1} (furanone C=O), 2883 cm^{-1} (N- CH_3)] and PYR [3414 cm^{-1} (asymmetric N-H stretching), 3288 cm^{-1} (symmetric N-H stretching), 3258 cm^{-1} (ν (=C-H) stretching), 1704 cm^{-1} (ν (C=O)), 1579 cm^{-1} (N-H bending, amine)] observed in ATR-FTIR spectra. The characteristic peaks for drugs were also reported in the physical mixture of polymers with drugs. Conclusively, we could confirm that no chemical modification observed as polymers mixed with drugs.

S3. Physicochemical characterization of nanoparticles

- *Particle size distribution and surface charge:* The hydrodynamic size (Z-average), polydispersity index (PDI), and electrokinetic potential (ζ -potential) of blank and ATD-loaded CSNP were computed using Zetasizer Nano ZS (Malvern Instruments, Worcestershire, UK). Prior to measurement, each formulation was diluted 1:10 (v/v) with Milli-Q water to evade multiple scattering.
- *Scanning Electron Microscopy (SEM):* The surface morphology of blank, ATD-loaded CSNPs and nano-aggregates was determined by SEM (JSM IT300LV, JEOL, Japan). CSNPs were evenly dispersed across silicon wafer and dried at room temperature. A silicon wafer was securely affixed to a metal stub using carbon tape and a fine coating of gold was meticulously applied onto the wafer using a coater (JEOL-3000FC, Japan). For measuring the shape of nanoparticles, secondary and backscattered electrons were collected under a microscope at 10.0 kV accelerated voltage.
- *Atomic Force Microscopy (AFM):* AFM analysis was conducted to validate the particle shape and size distribution of CSNP. The nanoparticles were drop-casted across silicon wafer and samples dried overnight at RT. Further, samples were analyzed at a scan rate of ~ 0.996 Hz under the AFM (Multimode 8 Nanoscope V, Bruker, USA). The AFM was set to tapping mode, and pictures were captured with a commercial RTESP silicon probe tip cantilever.

- *Transmission Electron Microscopy (TEM)*: The CSNPs sample was deposited on a carbon film backed by a 300-mesh copper grid via a drop-casting method, and samples were allowed to air dry at ambient temperature. Thereafter, the sample was observed using a JEOL JEM-2100, JEOL, Tokyo, Japan. The images were recorded by TEM at 120 kV of accelerating voltage.
- *Drug loading and Encapsulation efficiency*: Drug loading and encapsulation efficiency of drug-loaded CSNP were ascertained by separating CSNP from medium via centrifugation at 14000 rpm at 4°C for 30 min. The supernatant solution containing free INH and RIF were decanted and analyzed by UV-2600 spectrophotometer, Shimadzu, at 279 nm and 335 nm, respectively. The encapsulation efficiency was recorded as a percentage of the total ATD added. Each sample was tested in triplicate (n=3).

Table S1. Stability of prepared nano-in-microparticles following re-dispersion in simulated nasal fluid at an interval of 0 and 3 months on the particle size, polydispersity index (PDI), zeta potential and re-dispersibility index (RDI) of blank NA, INH-NA and RIF-NA formulations. Values are represented as mean \pm SD (n =3) of three individual measurements.

Formulations	Time (Months)	Particle size (nm)	Polydispersity index (PDI)	Zeta potential (mV)	Redispersibility index (RDI)
Blank-NA	0	174.2 \pm 1.7	0.136 \pm 0.08	15.1 \pm 0.7	1.03
	3	180.4 \pm 2.4	0.179 \pm 0.04	13.1 \pm 0.6	
INH-NA	0	188.2 \pm 2.7	0.185 \pm 0.03	14.2 \pm 1.1	1.08
	3	203.3 \pm 2.4	0.147 \pm 0.04	14.1 \pm 1.0	
RIF-NA	0	194.9 \pm 2.8	0.210 \pm 0.02	16.4 \pm 0.7	1.27
	3	248.4 \pm 4.4	0.226 \pm 0.01	13.7 \pm 1.0	

*All samples were in triplicate

S4. *In-vitro* drug release study

In vitro drug release investigations were performed using the dialysis bag technique [cellulose membrane, average flat width 10 mm (0.4 in.)] in a shaking water bath. Each ATD and ATD-NA powder was added in 2 mL of preheated simulated nasal electrolyte solution (SNES pH 5.5: NaCl-7.45 g/L, KCl-1.29 g/L, and CaCl₂-0.32mg/L). The dialysis bags (previously soaked overnight in milli-Q water) were then inserted into small screw-top glass vials containing 20 mL of phosphate buffer solution (PBS, pH 7.4), covered with Parafilm[®], and set in the water bath with gentle agitation at 35 \pm 0.2 °C. 200 μ L samples were extracted and replaced with equal volumes of fresh and preheated PBS solution at predefined time intervals (0, 5, 10, 15, 30, 45, 60, 120, and 240 min). INH and RIF levels in the samples were measured by UV-vis

spectrophotometer at 279 and 335, respectively. Experiments were repeated in triplicate (n=3). The release profile of ATD from prepared formulations were evaluated, and results are presented in figure 2. In case of INH-NA, the percentage INH release from INH-NA indicated controlled drug release from the formulation, with an initial burst release within an one hour (more than 30%) followed by a controlled release over 24 h under physiological conditions. In contrast, the release of RIF from RIF-NA particles showed a rapid release for an initial 3 h (more than 25%), followed by a sustained release of more than 71.98% over 24 h. The initial burst release of the drug may be attributed to the release of the drug from the surface of the NPs, while the sustained release was due to the constant release of drugs from the core of NPs caused by CS hydration and swelling[47].

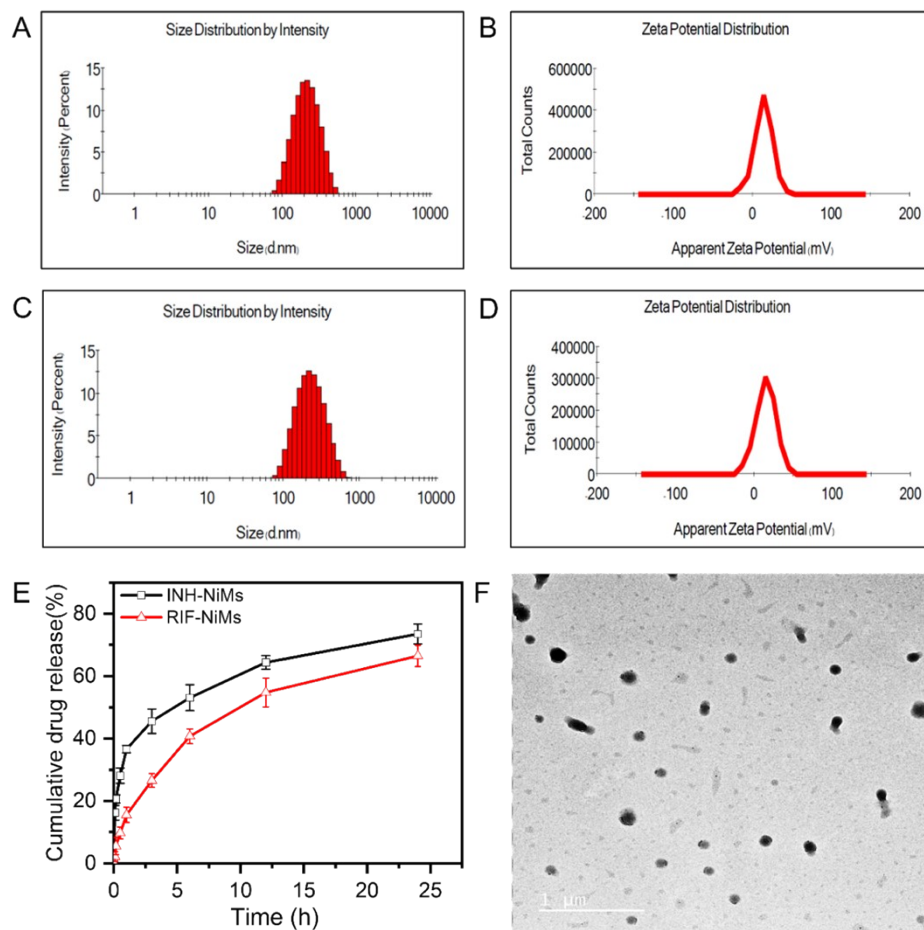


Figure S1. Particle size and (A) zeta potential (B) of INH-CSNP by dynamic light scattering (DLS). Particle size and (C) zeta potential (D) of RIF-CSNP by DLS. (E) In vitro release profile of INH-NA and RIF-NA using dialysis bag experiment. (F) Transmission electron microscopy (TEM) of redispersed CSNP. Data represents mean \pm S.D (n = 3).

S5. Physical stability studies

To assess the stability of spray-dried NA, a long-term physical stability study was conducted to scrutinize their performance under storage conditions. The NA were stored in tightly closed glass vials (n=3) protected from light and subjected to stability study at $25 \pm 2^\circ\text{C}$ temperature and $60 \pm 5\%$ relative humidity for a duration of 3 months. At a predetermined time point, NA were re-dispersed in SNES solution and characterized for morphology, particle size, PDI, and zeta potential as described in sections 2.3.1. Data were recorded as the mean \pm standard deviation (n=3).

Table S2. Physicochemical and aerodynamic properties of ATD-NA.

	Parameters	INH-NA	RIF-NA
Physicochemical properties	Mean diameter ($\mu\text{m} + \text{SD}$)	5.83 ± 1.97	6.45 ± 1.38
Aerodynamic properties	Emitted dose ($\% + \text{SD}$)	87.33 ± 4.61	81.87 ± 3.28
	MMAD ($\mu\text{m} + \text{SD}$)	6.58 ± 0.78	7.72 ± 0.59
	Fine Particle Fraction ($\% \pm \text{SD}$)	34.4 ± 4.22	31.46 ± 3.16
	Geometric Standard Deviation (μm)	1.77 ± 0.31	1.75 ± 0.17

Table S3. Flowability properties of prepared Blank-NA, INH-NA and RIF-NA

Formulation	Bulk density (g/cm^3)	Tapped density (g/cm^3)	Carr's Index (%)	Hausner ratio
Blank-NA	0.141	0.188	25.000	1.333
INH-NA	0.150	0.205	27.083	1.371
RIF-NA	0.181	0.258	29.730	1.423

S6. In vitro permeability study

Drug transport studies were performed using vertical Franz diffusion apparatus following the previously employed method. For the pre-treatment, regenerated cellulose membrane (Pore size- $0.45 \mu\text{m}$, Sartorius Stedim Biotech GmbH, Germany) was dipped in isopropyl myristate before investigations to mimic lipophilic nasal mucosa. Then, the membrane was mounted on diffusion cells (Orchid scientific & innovative Pvt. Ltd. Nashik, India) between the donor and acceptor phases and fixed with a metal clamp. The acceptor phase was filled with 20ml of PBS buffer (pH 7.4) and maintained at $35 \pm 0.5^\circ\text{C}$ throughout the experiment. This system was allowed to equilibrate for 15 min. Then, 10mg of INH, RIF, or equivalent INH-NA or RIF-NA were dispersed in 1ml SNES solution and added to the donor phase. At a specific time, interval from (0 to 4 h), an aliquot of 1ml from the acceptor phase was removed and replenished with fresh PBS to restore sink condition. The sample was analyzed using a spectrophotometer

at 279 and 335. The cumulative permeation ($\mu\text{g}/\text{cm}^2$) across the synthetic membrane was plotted against time, and the results were reported as the mean \pm SD ($n=3$).

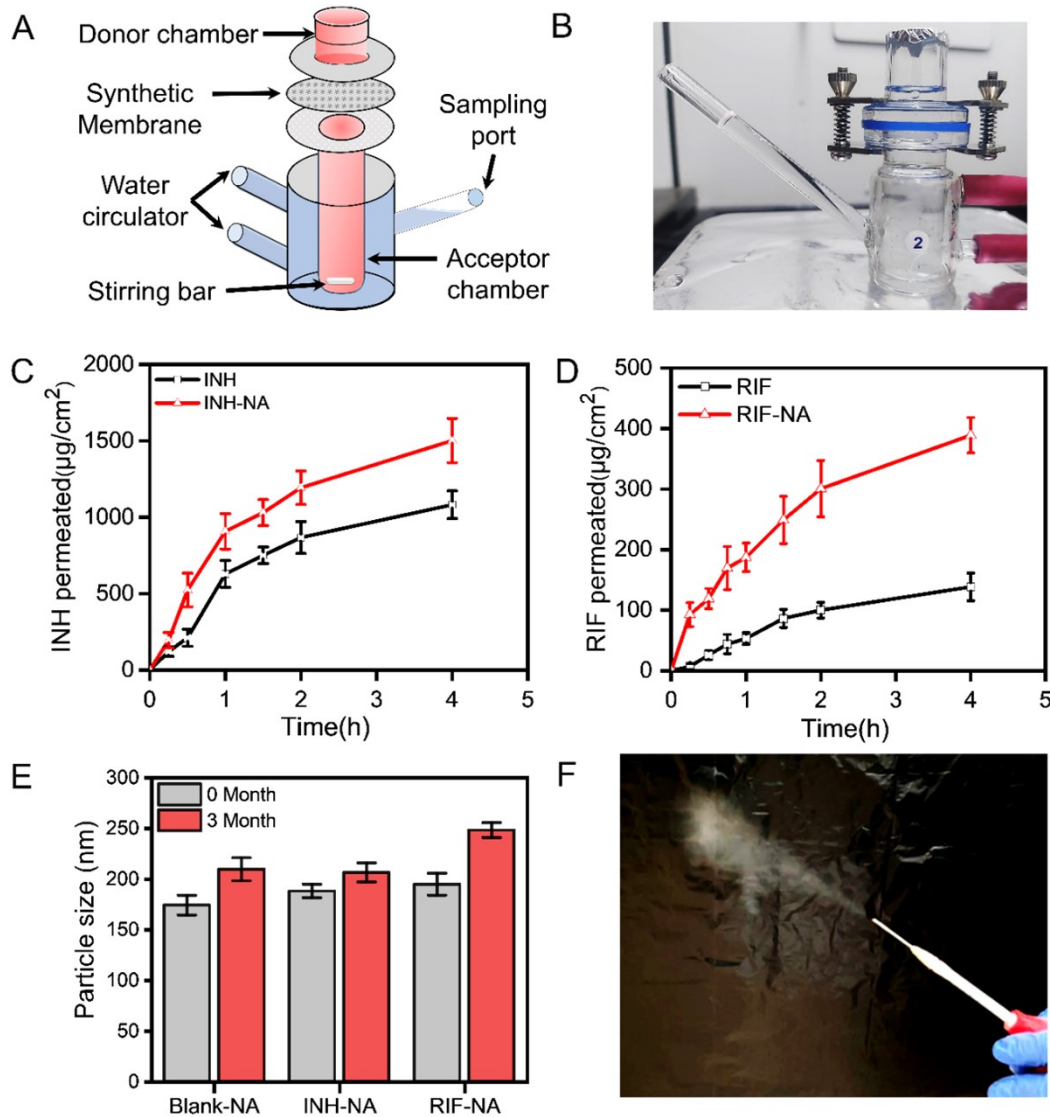


Figure S2. In vitro assessment of nasal diffusion through synthetic membrane and mucoadhesion strength of CSNP. (A) Schematic of Franz diffusion experiment. (B) Pictorial image of diffusion cells used for in vitro diffusion experiment. (C) Cumulative permeation of INH and INH-NA formulations across the RC membrane at different intervals. (D) Cumulative permeation of RIF and RIF-NA formulations across the RC membrane at different intervals. (E) Particle size changes occurred during storage conditions measured at 0 and 3 months. (F) The cloud of dry powder comprising ATD-NA emanates from the in-house designed device. Data represents as mean \pm S.D. ($n = 3$)

In vitro diffusion analysis of anti-TB drugs and their powder formulations was done through a regenerated cellulose which gives an idea of the relative permeation behaviour. The kinetic

measurements were recorded for a duration of 4 h, which exceeds the typical residence time of nasal formulations on the nasal mucosa, about 15 minutes. The cumulative permeation of drugs passing through the synthetic membrane is illustrated in figure 3C and 3D. The INH-NA powder formulation exhibited flux about $76.45 \mu\text{g}/\text{cm}^2/\text{min}$ of INH, while the bare INH had a slightly lower diffusion of $55.07 \mu\text{g}/\text{cm}^2/\text{min}$ following a 30 min interval. The higher permeation compared with bare INH owing to the higher solubility of INH resulted in a higher dissolution rate of the microparticles deposited on the membrane, governed the drug concentration in the donor and, consequently, the transport profiles across the membrane. The linearity of the release profiles throughout the initial hour signified the constancy of the gradient across the cellulose membrane, enabling the computation of the initial drug flux from the slope of the straight line. In the case of RIF-NA, the powder formulation also exhibited a significantly higher permeation rate with a flux of $19.80 \mu\text{g}/\text{cm}^2/\text{min}$, compared to the bare drug with a permeation of $7.05 \mu\text{g}/\text{cm}^2/\text{min}$. This enhanced diffusion may be attributed to the nano-encapsulation of anti-TB drugs as compared to raw RIF drugs.

S7. Fabrication of in-house nasal insufflation device

The custom-made device utilized in our experiments is a specialized insufflation device consisting of a glass tube integrated with a blunt-end needle and a hand pump. This device offers adaptability by allowing the use of needles with varying gauges based on the particle size of the formulations being administered. The inclusion of a hand pump enables convenient single-handed operation, which proves advantageous when applying the formulation to the rat's nose while simultaneously holding the rat with the other hand. The device's design provides flexibility during in vivo experiments, facilitating accurate and controlled delivery of the formulation to the desired target site.

The nasal powder-loaded exit diffuser of the device was carefully inserted into each nostril of the mice. Subsequently, the plunger of the syringe, containing a volume of 1 ml of air, was pressed down to initiate the release of a powder plume consisting of the ATD-NA powder into the nasal cavity. This method of intranasal administration was designed to ensure accurate and consistent delivery of the nasal powder into the nasal cavity of the animals. Prior to intranasal administration, a pre-determined quantity of powder was added to the insufflation device. The mice in the cohort were placed in a supine position, and the powder was puffed into each nare via the insufflator, with the animals remaining in this position for 30 seconds. The amount of

powder released after each actuation was calculated by measuring the weight of the device before and after powder insufflation (Emitted dose: ~ 90%).

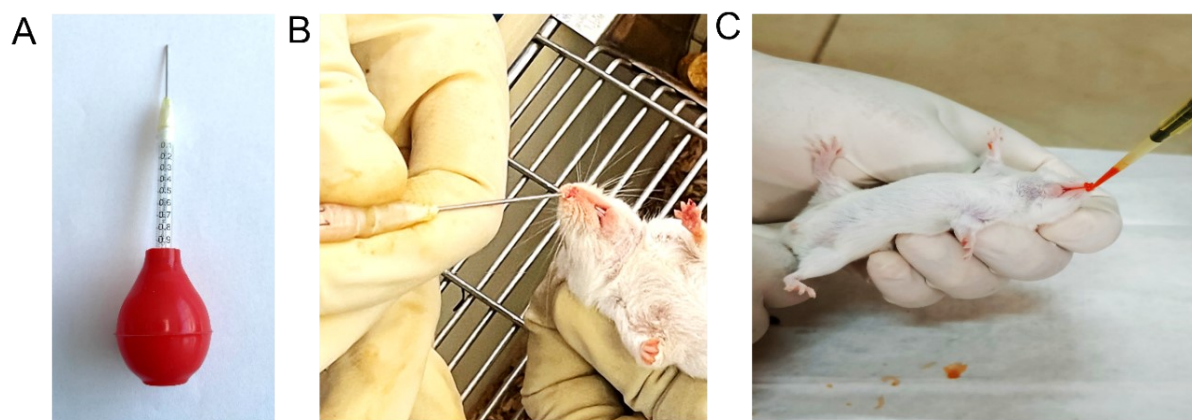


Figure S3. Nasal administration of mice. (A) ATD-NA dry powder cloud evolving from the nasal dry powder delivery device prepared in house. Pictorial representation of nasal administration of powder using in house prepared insufflator (B) and instillation (C).

S8. Pharmacokinetic study

The concentration of ATD in the brain after intranasal administration of ATD-MP was studied using BALB/c mice. The animals were divided into two groups, with each group containing six mice. The first group received oral administration of INH and RIF at a dose of 250 μ g/mice and 625 μ g/mice, respectively, via oral gavage. The second group received intranasal administration of ATD-NA dry powder containing the same dose of INH and RIF via an insufflation device designed to generate a puff of powder for N2B delivery. The treatment was administered for five days a week for a duration of three weeks. Blood samples were collected at predefined intervals of 0.5, 1, 6, and 12 hours after administration, and brain samples were also harvested for drug content analysis. The results were analyzed to determine the C_{max} , t_{max} , and the area under the curve of the pharmacokinetic profile. All experiments were conducted in compliance with guidelines set by the Institutional Animal Ethics Committee and all safety precautions were taken to prevent aerosol generation.

• *Sample preparation and drug quantification by HPLC*

In order to analyze the presence of INH and RIF in tissue homogenates and blood serum, various solvent systems were employed. To extract INH, a modified version of the procedure by Verma et al was used. Initially, a solution of 20% (wt/vol) NaCl was added to the tissue homogenate or serum, followed by extraction with a chloroform-butanol (70:30, vol/vol)

solvent system. The mixture was vortexed for 1 minute and centrifuged at 4,000 g for 10 minutes. This process was repeated three times, and the pooled supernatants were then extracted for INH by adding 0.5 ml of 30 mM phosphoric acid. RIF was extracted from the tissue homogenates and serum by using a solvent system comprising equal parts of dichloromethane and n-pentane. Butylated hydroxytoluene (BHT) dissolved in acetonitrile was added to the samples at a final concentration of 0.1% (wt/vol) to minimize drug degradation. The samples were vortex mixed for 1 minute and centrifuged at 2,604 g for 10 minutes, followed by vacuum drying and reconstituting in 500 µl of methanol before being filtered through a 0.22 µm filter just prior to injection.

A rapid and sensitive HPLC-UV method was used to determine the INH and RIF in tissue homogenates. HPLC was performed on an iUHPLC-3000PLUS system (Analytical Technologies Limited, India) equipped with an autosampler (L-3400), quaternary pump (L-3245), and UV-vis detector (L-3500). Separation was achieved using a ZOBRA[®] Eclipse Plus C18 column (4.6 mm x 250 mm, 5 µm; Agilent Technologies). The mobile phase and other analytical parameters were presented in Table. S4

Table S4. HPLC parameters for method development and validation

Parameters	INH	RIF
Column	C18- 250 x 4.60 mm, 5 µm	C18- 250 x 4.60 mm, 5 µm
Mobile Phase	0.01 M phosphoric acid: acetonitrile (ACN)	Acetonitrile (ACN): Phosphate buffer (pH 6.5)
Ratio	90:10	45:55
Detector	UV-vis detector	UV-vis detector
Run time	10 Minutes	15 Minutes
Wavelength (λ_{\max})	205 nm	335 nm
Flow rate	1 mL/min	1 mL/min
Injection Volume	20 µL	20 µL

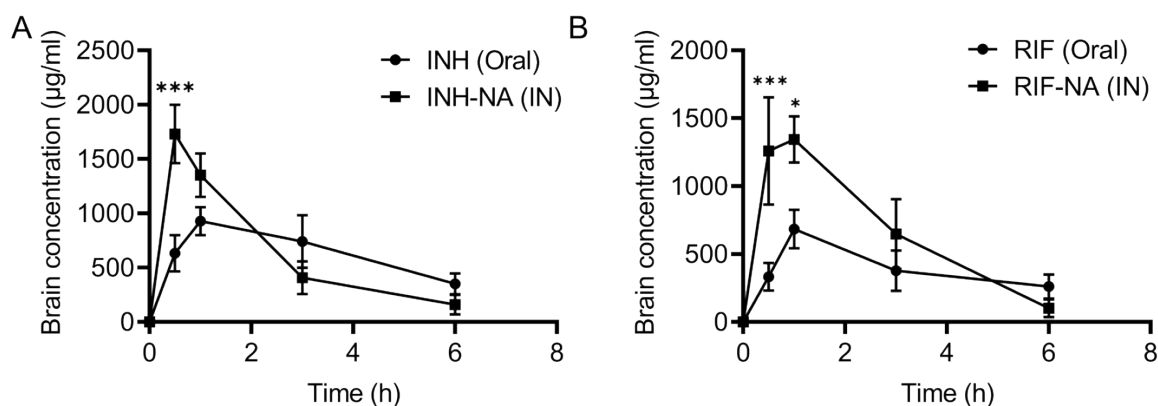


Figure S4. Pharmacokinetics and tissue distribution of single intranasal dose of ATD-NA and oral dose of ATD. (A) The concentration-time profile of INH and RIF in the brain homogenates. The results expressed as mean \pm SD.

Table S5. Selected pharmacokinetic parameters of ATD-NA delivered via the oral and intranasal routes in the brain homogenate of mice (All samples were expressed as mean \pm SD)

Pharmacokinetic parameters	INH conc. in brain homogenate		RIF conc. in brain homogenate	
	Oral	Intranasal	Oral	Intranasal
$t_{1/2}$ (h)	3.48	1.58	3.68	1.32
T_{max} (h)	1.0	0.5	1.0	1.0
C_{max} (ng·ml ⁻¹)	927.3	1730.6	513.3	1008.5
$AUC_{(0-t)}$ (ng/ml·h)	3851.7	3807.9	1768.0	3061.4
$AUC_{(0-\infty)}$ (ng/ml·h)	5618.5	4170.7	2805.9	3206.6

Note: $t_{1/2}$ = biological half-life; T_{max} = Observed time to reach peak concentration; C_{max} = observed peak concentration; $AUC_{(0-t)}$ = the area under the concentration-time curve from time '0 to t'; $AUC_{(0-\infty)}$ = the area under the concentration-time curve from time zero extrapolated to infinity.

Pharmacokinetic investigations were conducted on mice to evaluate the potential of ATD-NA to enhance nasal bioavailability through intranasal administration compared to oral administration. The concentration-time profiles of INH and RIF in the brain homogenate following both administration routes are illustrated in Figure S4. The brain concentration-time plots (Figure S4) revealed that the time to reach maximum concentration (T_{max}) of INH in the brain was shorter for the intranasal INH-NA group (0.5 h) compared to the oral INH group (1 h). This indicates a more rapid permeation of formulated INH through the nasal mucosa into the brain via the nasal cavity. The maximum concentration (C_{max}) of INH in the brain was significantly higher in the intranasal INH-NA group (1730.6 ng/ml) compared to the oral INH group (927.3 µg/ml).

The brain concentration-time plots (Figure S4) revealed that the time to reach maximum concentration (T_{max}) of INH in the brain was shorter for the intranasal INH-NA group (0.5 h)

compared to the oral INH group (1 h). This indicates a more rapid permeation of formulated INH through the nasal mucosa into the brain via the nasal cavity. The maximum concentration (C_{max}) of INH in the brain was significantly higher in the intranasal INH-NA group (1730.6 ng/ml) compared to the oral INH group (927.3 μ g/ml). Similarly, the brain concentration-time plots (Figure S4) revealed that the T_{max} of RIF in the brain was similar for the intranasal RIF-NA group and the oral INH group. However, the C_{max} of RIF in the brain was significantly higher in the intranasal RIF-NA group (1008.5 ng/ml) compared to the oral INH group (513.3 μ g/ml). This indicates a more rapid permeation of formulated RIF through the nasal mucosa into the brain via the nasal cavity. The AUC values following intranasal administration of RIF-NA were ~2 times higher than those observed with oral RIF treatment (Table S5). These results indicate that intranasal administration of ATD-NA leads to significantly increased drug exposure and distribution in the brain, effectively bypassing the blood-brain barrier (BBB). These findings suggest that a substantial portion of antibiotics directly enters the brain via olfactory and trigeminal neural pathways following intranasal administration, rather than through the bloodstream.

References

M. Fazil, S. Md, S. Haque, M. Kumar, S. Baboota, J. kaur Sahni, J. Ali, Development and Evaluation of Rivastigmine Loaded Chitosan Nanoparticles for Brain Targeting, *European Journal of Pharmaceutical Sciences*, 47 (2012) 6-15. <http://dx.doi.org/10.1016/j.ejps.2012.04.013>